Available online at www.sciencedirect.com

ScienceDirect

Procedia - Social and Behavioral Sciences 186 (2015) 1087 – 1094

Procedia
Social and Behavioral Sciences

5th World Conference on Learning, Teaching and Educational Leadership, WCLTA 2014

The Influence of Wind on the Pantograph Placed on the Railway Electric Vehicles Bodywork

Sorin Arsene[a]*, Ioan Sebesan[a], Gabriel Popa[a]

[a]*University POLITEHNICA of Bucharest, Department of Railway Rolling Stock, Splaiul Independenţei 313, 060042, Bucharest, Romania*

Abstract

The winds gusts with high speed can negative affect the operation of railway electric vehicles. These vehicles can achieve high performances, as long as the power supply is ensured, without discontinuities or interruptions in the process. This article is an analysis of how the wind gusts affect variation drag resistance to advancing caused by the pantograph and how they affect the supply of electricity required for vehicle movement. To this end, in a first step, we modeled geometrically in 3D EP3pantograph, which was raised to maximum working height. For simulation of air flow among the components of the collector (pantograph active) we considered how it is used and placed on the vehicle body. For analyze the effects caused by gusts of wind, we considered point values for angles within the range [0°, 180°] and speeds, a range of from 0 m/s to 30 m/s. This article is developed in programs postdoctoral studies at the University Politehnica of Bucharest.

Peer-review under responsibility of Academic World Education and Research Center

Keywords: pantograph; gusts of wind; air flow simulation;

1. Introduction

Electric railway vehicles it can moves between two points located on a section of a railroad when the energy required for this purpose is taken from an external source, in this case line of contact (catenary). The equipment, through which a vehicle is supplied with energy from catenary is called the pantograph and is located on its body. The placement and use of the collector (pantograph) determine an increasing on the resistance to moving and hence the energy required to moving the electric vehicle compared to a vehicle powered from an internal source of energy

*Assist. Prof. PhD eng. Sorin Arsene. Tel.: 004.021.402.96.95.
E-mail address: sorinarsene@gmail.com

Peer-review under responsibility of Academic World Education and Research Center
doi:10.1016/j.sbspro.2015.04.185

(diesel vehicle), as can be seen and in papers (Arsene, 2013; Sebeșan, Arsene & Stoica, 2013; Sebeșan, Arsene & Stoica, 2013; Sebesan & Arsene, 2014; Raghunathan, Kim & Setoguch, 2002).

In normal condition to moving of the electric rail vehicles, these must overcome, drag resistance to advancing. Resistant forces are determined by a number of frictions such as: the bearings of axles; by rolling and / or sliding of the wheels and the road surface; with the air; (Lukaszewicz, 2001).

Drag resistances are generated by the vehicle's own speed and by the variation of wind speed

In Romania, according to the data measured by the National Institute of Meteorology and Hydrology (NMA), the highest wind speed values were reached in February 1954 in Bucharest and at Iasi in winter of 1966, these being of 126km/h respectively 200km/h.

Generalized formula for determining the running resistance for railway vehicles also is known as Davis's relationship (Lukaszewicz & Andersson, 2009; Sebesan & Arsene, 2012; Arsene, 2013; Sebesan & Taruș, 2011), is:

$$R_t = a + b \cdot v + c \cdot v^2 \tag{1}$$

Where: R_t - Total resistance to motion of the vehicle; a - Mechanical rolling resistances caused by the axle loads; $b \cdot v$ - Non-aerodynamic drag; $c \cdot v^2$ - Aerodynamic drag; v - Speed of the vehicle.

Explicit formula for the parameter "c" regarding aerodynamic resistances according to the literature (Anderson Jr., 1991; Sebesan & Țaruș, 2012; LI, Dong, JI & Zhang, 2012; Cheli, Ripamonti, Rocchi, & Tomasini, 2010; Cheli, Corradia, Rocchia, Tomasinia, & Maestrinib, 2010; Schobera, M.Weisea, Orellanoa, Deegb, & Wetzelc, 2010) is:

$$c = \frac{C_x \cdot S \cdot \rho}{2} = \frac{\frac{2 \cdot F_x}{\bar{v}^2} \cdot S \cdot \rho}{2} \quad \text{„} \tag{2}$$

Where: C_x - Aerodynamic coefficient of air sliding (also known as the coefficient of air penetration); S - Front surface of the vehicle in cross section (m^2); ρ - density of the moving vehicle air (kg/m^3); F_x - the frontal sliding force (N); $\bar{v}$ - velocity of the fluid (air) (m/s).

2. Resistance of the pantograph and influence of wind on its

The placement and positioning of active pantograph on the vehicle body, causes two distinct modes of its use. These two situations are determined by the position of the joint of the arms pantograph as follows: a) when joint of the arms pantograph determine an angle pointing to the air flow direction opposite to the direction of travel of the vehicle (Fig. 1.a); b) When the joint between the lower and upper pantograph arm has the peak of angle oriented in the opposite of air flow, indicating the direction of travel of the vehicle (Fig. 1.b)

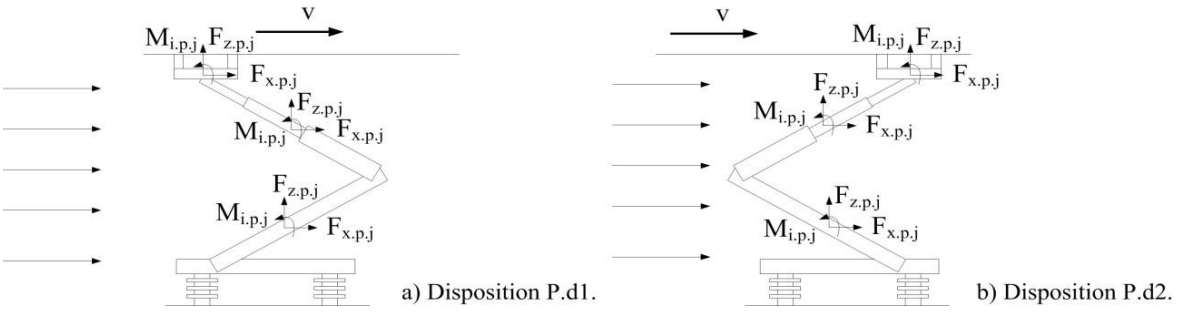

Fig. 1.a-b Modes of the pantograph arrangement.

The drag resistance generated by the collector current can be determinate on based on the study of equilibrium of forces and moments acting on the components of the pantograph as is presented in article (Pombo, Ambrósio, Pereira, Rauter, Collina, & Facchinetti, 2009). Under this method the aerodynamic forces acting on the pantograph components are evaluated based on the corresponding aerodynamics coefficients as follows:

$$F_{xpj} = \frac{\rho \cdot \left(C_x \cdot S_p\right)_j \cdot v_{rel.p}^2}{2} \tag{3}$$

$$F_{zpj} = \frac{\rho \cdot \left(C_z \cdot S_p\right)_j \cdot v_{rel.p}^2}{2} \tag{4}$$

$$M_{ipj} = \frac{\rho \cdot \left(C_{mi} \cdot S_p \cdot l_p\right)_j \cdot v_{rel.p}^2}{2} \tag{5}$$

where: i – index on axis Cartesian coordinate system; j – index of the components of the pantograph; F_{xpj}, F_{zpj} – Aerodynamic forces in the longitudinal direction and vertical to each element of the pantograph; M_{ipj}– Moments for each axis of the Cartesian system determined on the components of the pantograph; $v_{rel.p}$ –relative incidence speed of fluid flow among pantograph elements; $C_x \cdot S_p$, $C_z \cdot S_p$ și $C_{mi} \cdot S_p \cdot l_p$ – pressure coefficients of the aerodynamic frontal resistance respectively that vertical and couples resulted for each element j in witch was divided pantograph.

Determination of relative rate (relation 6), depends on the direction and angle in witch blows the wind to the longitudinal axis of the vehicle is shown in Fig. 2.

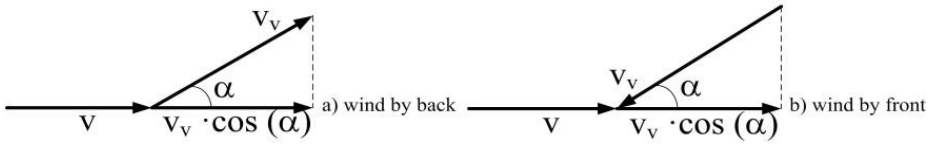

Fig. 2.a-b The influence of the wind on the angle and direction its.

$$v_{rel} = v + v_v \cdot \cos(\alpha) \tag{6}$$

Where v – speed of the vehicle; v_v – wind speed; α – angle between the direction of movement of the vehicle and the speed of the wind.

In this condition the aerodynamic force coefficients (relation 7) and moments (relation 8) generated by the flow of air through the pantograph elements can be written as:

$$C_{ij} = \frac{2 \cdot F_{ipj}}{S_{pj} \cdot \rho \cdot v_{rel}^2} = \frac{2 \cdot F_{ipj}}{S_{pj} \cdot \rho \cdot \left(v + v_v \cdot \cos(\alpha)\right)^2} \tag{7}$$

$$C_{mij} = \frac{2 \cdot M_{ipj}}{S_{pj} \cdot l_{ij} \cdot \rho \cdot v_{rel}^2} = \frac{2 \cdot M_{ipj}}{S_{pj} \cdot l_{ij} \cdot \rho \cdot \left(v + v_v \cdot \cos(\alpha)\right)^2} \tag{8}$$

When the wind speed is geared towards the train movement (wind from behind), decreases air resistance or has a negative value. Negative values occur only when the speed component the equivalent determined by wind is greater

than the speed of movement of the vehicle and has the same direction as the direction of travel thereof, as described in the paper (Gregoire, Collina, Resta & Rocchi, 2008).

3. Simulation of air flow through the pantograph elements

For simulation we considered the case determined by the design of the EP3 pantograph, which is used in a majority of LE 060 EA 5100kW electric locomotives, located in the park of the railway companies operating in Romania.

Geometric modelling of the pantograph at scale 1:1 was made using Autodesk Inventor. With these components, I realized assembly of the pantograph so that its patina by located at the height allowable maximum 2.5m for capture of the current, according to its technical specification.

In order to simulate the air flow through the components of the pantograph I used SolidWorks Flow Simulation software. It uses the flow equations Navier-Stokes Favre mediation model and for closing the system of equations in the turbulent regime is use k-ε model.

In this paper, I considered for analysis the two cases on arrangement of the active pantograph (fig. 1), where we took into account the relative velocity of the air when the vehicle is moving at a constant speed of 144km/h = 40m/s.

In terms of wind speed, for this, we took successive values of 0m/s and 10m/s, 20m/s, respectively 30m/s. For angle between of wind direction and the direction of movement of the vehicle, we considered successively cases: 0^o, 30^o, 45^o, 60^o, 90^o, 120^o, 150^o, 180^o. Under these conditions resulted 50 distinct cases for analyse.

The delimitation of the volume of air flow is carried out as follows: Vertical we considered the appropriate plan of the vehicle roof and another plan to 6 m of it; The cross section, we considered two plans located symmetrically at 5 m from the longitudinal plane of the vehicle; The longitudinal section, we considered two planes located at 5 m and 10 m, the transverse plane of the pantograph frame. First plan of longitudinal sections (5 m) corresponds to the front of the locomotive in air flow direction and the second plan of the same sections (10m) at the back of the vehicle.

As input parameters regarding atmospheric conditions, we consider of pressure and temperature values: 101325 Pa for pressure and 293.2 K for temperature.

In the Fig. 3 are presented dynamic pressure variation during simulation when do not act on it and speed variation caused by wind.

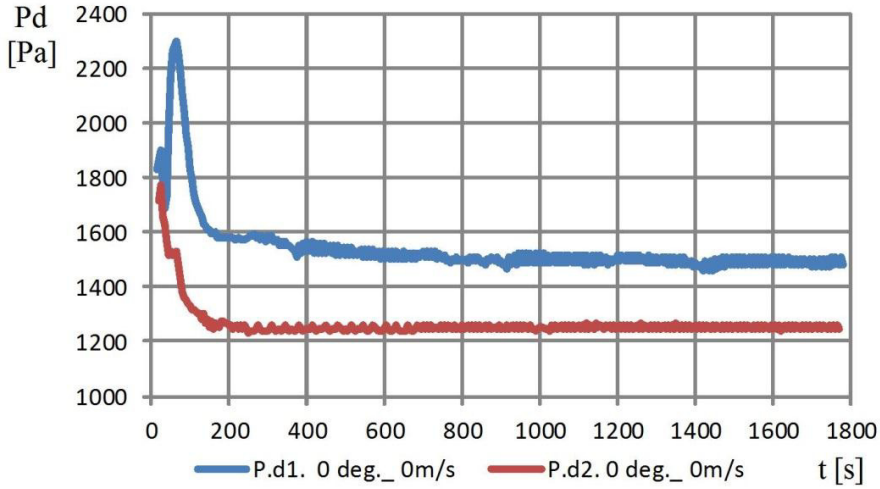

Fig. 3. Variation of the dynamic pressure during simulation from around pantograph when we have not wind gusts

For situations when on pantograph acts additional and wind speed, dynamic air pressure variation obtained by simulation are shown in Fig. 4.

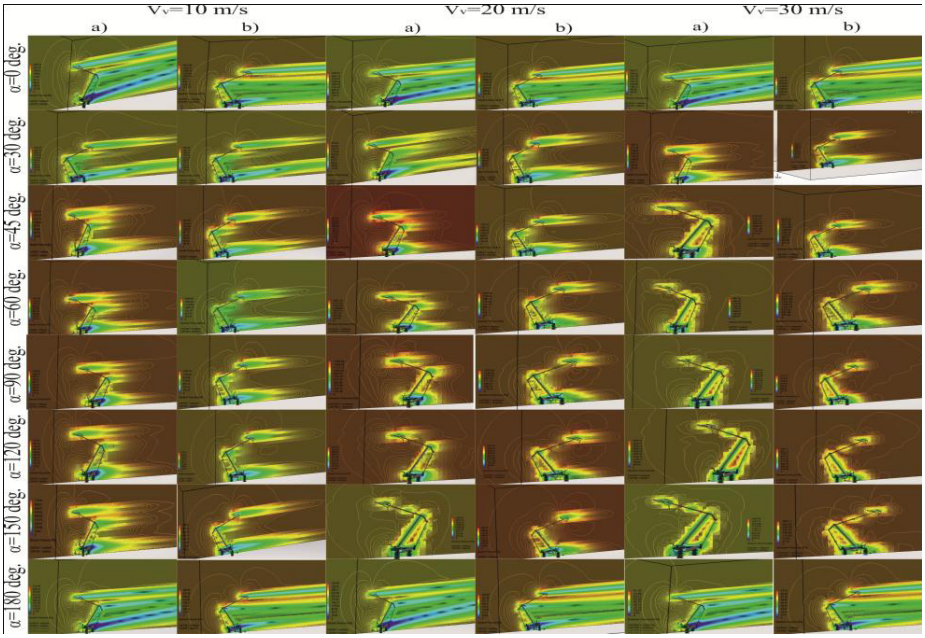

Fig. 4. Counters lines of the dynamic pressure.

Aerodynamic resistance values obtained on the basis the air flow simulation of the analyzed cases are shown in Figure 5 taking into account the 8 values of the angles.

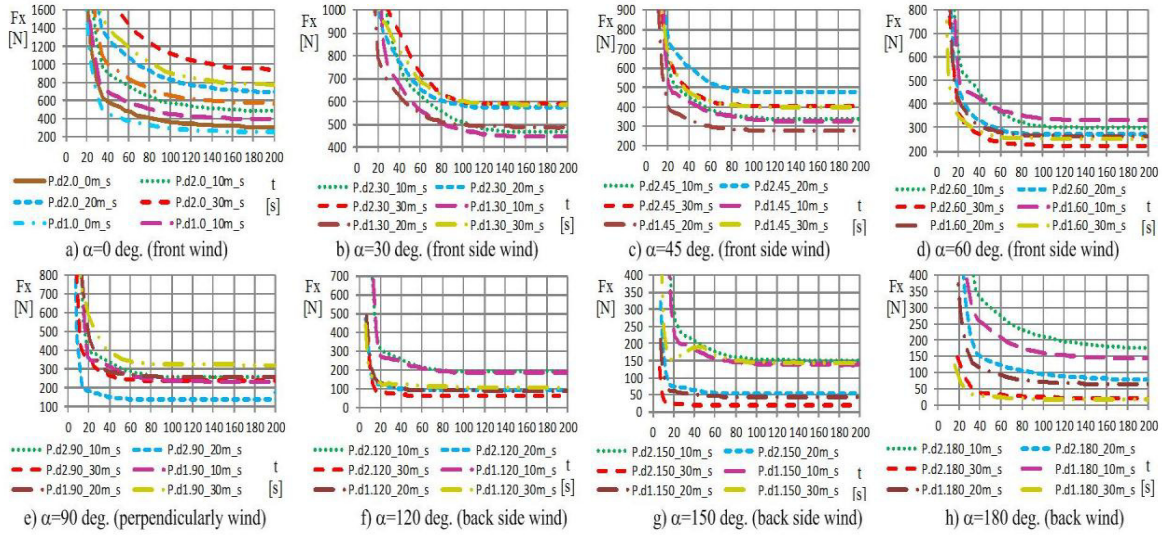

Fig. 5. Variation aerodynamic resistance during simulation for the 8 values of the angles of wind.

Evaluation the influence of wind on aerodynamic drag generated by pantograph we performed an analysis of the percentage fixed values obtained from simulations. We are considering successively as a landmark three types of values: when the vehicle moves in atmospheric conditions without wind gusts (Fig. 6); the wind speed is 10 m / s (Fig. 7); the wind speed is front (Fig. 8).

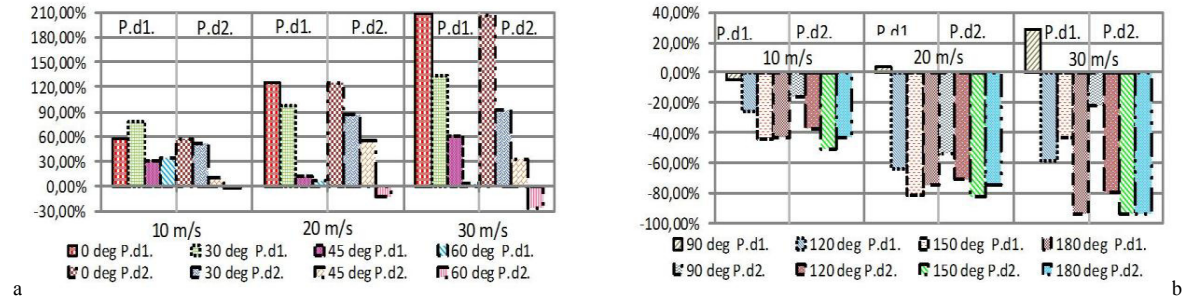

a b

Fig. 6. a-bThe percentage analysis of aerodynamic drag generated by the pantograph, having as benchmark, resistance obtained when the vehicle is moving under atmospheric conditions without the wind gusts.

Stabilized values by the aerodynamic drag of the pantograph resulting from the simulations are presented in Table no 1 for first disposition mode (P.d1.), respectively on Table no 2 for second disposition mode (P.d2.).

Table 1. Stabilized values of the aerodynamic drag to pantograph Fx[N] disposition mode P.d1.

Ungle v_v[m/s]	0°	30°	45°	60°	90°	120°	150°	180°
0	247,72 [N]	-	-	-	-	-	-	-
10	388,43 [N]	443,55 [N]	322,63 [N]	331,81 [N]	235,27 [N]	182,83 [N]	138,04 [N]	140,37 [N]
20	558,78 [N]	487,15 [N]	276,09 [N]	265,47 [N]	256,38 [N]	88,43 [N]	44,71 [N]	61,81 [N]
30	762,27 [N]	576,98 [N]	398,87 [N]	254,63 [N]	319,54 [N]	102,66 [N]	138,83 [N]	15,55 [N]

Table 2. Stabilized values of the aerodynamic drag to pantograph Fx[N] disposition mode P.d2.

Ungle v_v[m/s]	0°	30°	45°	60°	90°	120°	150°	180°
0	306,80 [N]	-	-	-	-	-	-	-
10	478,49 [N]	462,71 [N]	334,99 [N]	298,74 [N]	256,75 [N]	190,04 [N]	149,99 [N]	174,26 [N]
20	689,54 [N]	572,73 [N]	474,59 [N]	270,12 [N]	140,31 [N]	89,82 [N]	53,01 [N]	77,37 [N]
30	937,71 [N]	589,83 [N]	405,68 [N]	224,67 [N]	238,87 [N]	62,20 [N]	19,11 [N]	19,30 [N]

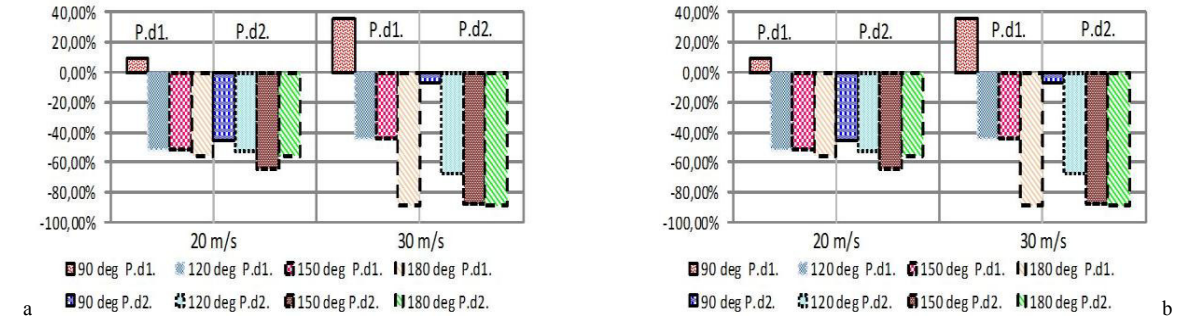

a b

Fig. 7. a-bThe percentage analysis of aerodynamic drag generated by the pantograph, having as benchmark, the resistances obtained for a wind of 10m / s corresponding to each angle considered.

Taking as a benchmark for comparison, the lowest wind speeds for the angles examined (Fig. 7), it is found that the extreme values, for the percentage variation to aerodynamic drag of the pantograph are obtained also for $\alpha=0^o$ – $v_v=30m/s$ ($\approx 96\%$) - the maximum increase, respectively for $\alpha=180^o$ – $v_v=30m/s$ ($\approx -89\%$) - maximum decrease.

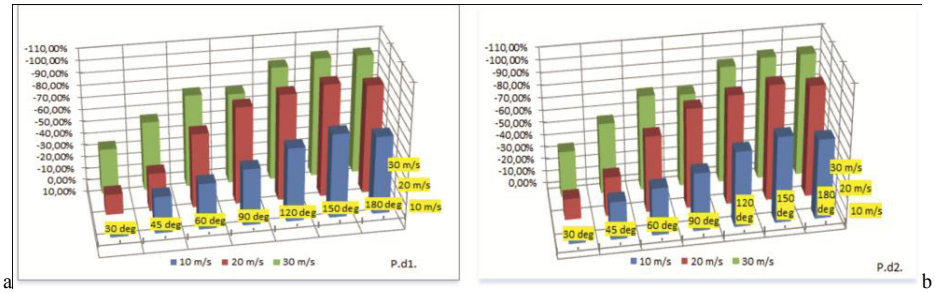

a b

Fig. 8. a-b The percentage analysis of aerodynamic drag generated by the pantograph, having as benchmark, the resistances to a frontal wind.

Comparing with the situation when the wind is in the front (Fig. 8) points out that in this situation are obtained the biggest aerodynamic drag generated by the pantograph, implicitly they will cause consume on higher energy

4. Conclusions

Appearance of wind gust and variation of its velocity influences on the exerted pressure values on the pantograph and by default to the aerodynamic drag thereof. From figure 5a to figure 5h it can see that: the extreme values stabilized results after simulation with respect to the aerodynamic drag of the pantograph is obtained in case of the high wind speeds. When the wind is oriented against the direction of travel of the vehicle (wind from the front), we obtain the maximum value of resistance. If it is oriented the direction of travel (wind from behind) result the minimum values of resistance. This sweeping is leading to changes in corresponding mod to the electricity consumed by the vehicle.

In the range of values considered to be the angle (0^o – 180^o) formed between the wind direction and the longitudinal axis of the vehicle, considering the constant speed thereof, it follows that the stabilized values of the aerodynamic drag the pantograph have a tendency decreasing with the increase thereof. For situations where it is considered a constant angle and wind speed variation, the simulations has resulted in a random distribution values of the aerodynamic drag the pantograph. This distribution starts at a rising trend of resistance with the speed, in the case of the front wind, and reach up to trend decreasing with this when the wind blows from behind.

In the first two comparative percentages analysis, regarding the aerodynamic drag of the pantograph (Fig. 6, Fig. 7), reveals that, in the range between 0° and 90° for angle α obtained largely positive. This means that wind gusts determines an increase of the aerodynamic resistance. For the rest of interval from 90° to 180°, the values are mostly negative, which means a reduction in aerodynamic drag. Changing wind speed and of the angle in which beats this, determines the change of aerodynamic resistances of pantograph, implicitly of the vehicle. This in turn causes further variation of the amount of energy required to move the locomotive.

Acknowledgements

This work is supported by the Sectorial Operational Programme Human Resources Development (SOP HRD), financed from the European Social Fund and the Romanian Government under the contract number POSDRU/159/1.5/S/137390

References

Anderson J. D. Jr. (1991). Fundamentls of aerodynamics – Second Edition. Ed. McGraw-Hill.

Arsene, S., (2013). Analysis regarding the aerodynamic resistances on boxes electric locomotives. *The International Conference on INnovation and Collaboration in Engineering Research – " INCER 2013",* (pp. 157-160). Bucharest,

Arsene, S., (2013). *Teză de Doctorat - Contribuţii privind îmbunătăţirea performanţelor de tracţiune ale vehiculelor electrice.* Bucureşti: Universitatea Politehnica din Bucureşti.

Cheli, F., Corradia, R., Rocchia, D., Tomasinia, G., Maestrinib, E., (2010). Wind tunnel tests on train scale models to investigate the effect of infrastructure scenario. *Journal of Wind Engineering and Industrial Aerodynamics, 98*(6-7), 189–201.

Cheli, F., Ripamonti, F., Rocchi, D., Tomasini, G., (2010). Aerodynamic behaviour investigation of the new EMUV250 train to cross wind. *Journal of Wind Engineering and Industrial Aerodynamics, Volume 98*(Issues 4–5), Pages 189–201.

Gregoire, R., Collina, A., Resta, F., Rocchi, D.,(2008). Some considerations on the aerodynamics of high speed pantograph: cfd and wind tunnel tests. BBAA VI International Colloquium on: Bluff Bodies Aerodynamics & Applications. Milano, Italy.

LI, L, Dong, W., JI, Y., Zhang, Z. , (2012). A minimal-energy driving strategy for high-speed electric train. *J Control Theory, 10*(3), 280–286.

Lukaszewicz, P., Andersson. E.,(2009). Green Train energy consumption Estimations on high-speed rail operations. Stockholm: KTH Railway Group. Retrieved from http://www.kth.se/polopoly_fs/1.179876!/Menu/general/ column-content/attachment/GT%20Energy%20consumption%20slutl.pdf

Lukaszewicz, P., (2001). Doctoral Thesis - Energy Consumption and Running Time for Trains - Modelling of running resistance and driver behaviour based on full scale testing. Stockholm: Department of Vehicle Engineering Royal Institute of Technology, KTH.

Orellano, A., Schober, M., (2006). Aerodynamic Performance of a Typical High-Speed Train. Proceedings of the 4th WSEAS International Conference on Fluid Mechanics and Aerodynamics, (pp18-25). Elounda, Greece.

Pombo, J., Ambrósio, J., Pereira, M., Rauter, F., Collina, A., Facchinetti, A.,(2009,). Influence of the aerodynamic forces on the pantograph–catenary system for high-speed trains. *Vehicle System Dynamics, Vol. 47*,(No. 11,), 1327–1347.

Raghunathan, R. S. , Kim, H.-D. , Setoguch, T.,(2002). Aerodynamics of high-speed railway train. *Progress in Aerospace Sciences, no.* 38, (Iss .6–7), 469–514.

Schobera, M., Weisea, M., Orellanoa, A., Deegb, P., Wetzelc, W. (2010). Wind tunnel investigation of an ICE3 endcar on three standard ground scenarios. *Journal of Wind Engineering and Industrial Aerodynamics, Volume 98*(Issues 6–7), Pages 345–352

Sebesan, I. , Ţarus. B., (2012). The impact of aerodynamics on fuel consumption in railway applications. *Incas Bulletin, Volume 4*(Issue 1), pp. 93 – 102.

Sebeşan, I., Arsene, S., Stoica, C., (2013). Experimental study on determination of aerodynamic resistance to progress for electric locomotive LE 060 EA1 of 5100 kW. *Scientific Bulletin-University Politehnica of Bucharest, Series D, 75*(4), p. 85-96.

Sebesan, I., Arsene, S., (2012). Considerations on study the aerodynamic of pantographs railway vehicles. *International Conference of Aerospace Sciences – "AEROSPATIAL 2012"*, (pp. 397-402). Bucharest.

Sebesan, I., Arsene, S., (2014). Study on aerodynamic resistance to electric rail vehicles generated by the power supply. papers selected to be published in the *Special Issue, Incas Bulletin,, 6*(Special Issue 1), 151 – 158. doi:http://dx.doi.org/10.13111/2066-8201.2014.6.S1.17

Sebeşan, I., Arsene, S., Stoica, C., (2013). Experimental analysis for aerodynamic drag of the electric locomotives. *Incas Bulletin, 5*(3), pp.99-115. doi:DOI: 10.13111/2066-8201.2013.5.3.11

Sebesan, I., Tarus, B., (2011). Some aspects regarding the impact of aerodynamics on fuel consumption in railway applications. *U.P.B. Sci. Bull., Series D, Vol. 73*(Iss. 4), pp 237-246.